

Linking Carbon Saturation Concepts to Nitrogen Saturation and Retention

Michael J. Castellano,^{1,2*} Jason P. Kaye,² Henry Lin,² and John P. Schmidt³

¹Department of Agronomy, Iowa State University, 2101 Agronomy Hall, Ames, Iowa 50011, USA; ²Department of Crop and Soil Sciences, The Pennsylvania State University, 116 ASI Building, University Park, Pennsylvania 16802, USA; ³USDA-ARS PSWRMU, University Park, Pennsylvania 16802, USA

ABSTRACT

Recent advances in soil C saturation concepts have increased our understanding of soil C storage and mineralization without explicit links to N retention and saturation theories. Here, we exploit soil texture and organic matter (OM) gradients in a Maryland, USA hardwood forest to test hypotheses that link soil organic C saturation with soil ¹⁵N retention and nitrification. At our site, mineral-associated OM (MAOM) N concentrations in the silt + clay particle fraction (g MAOM-N g silt + clay⁻¹) were negatively correlated with the fraction of NH₄-N transferred to MAOM during a 3-day in situ incubation ($R = -0.85$), but positively correlated with potential net nitrification ($R = 0.76$). Moreover, the fraction of NH₄-N transferred to MAOM was negatively correlated with potential net nitrification ($R = -0.76$). Due to physico-chemical stabilization mechanisms, MAOM is considered to be resistant to mineralization. Carbon saturation theory suggests that the proportion of new C inputs that can be stabilized in MAOM

decreases in proportion to the amount of C already present in the fraction; C inputs not stabilized in MAOM are susceptible to rapid mineralization. We demonstrate that NH₄-N stabilization in MAOM is similar to C stabilization in MAOM and associated with nitrification, thereby extending soil C saturation theory to mineral N and linking it with N retention and saturation theories. These data and concepts complement N saturation models that emphasize vegetation type, N input levels, and microbial turnover. Incorporating the OM retention capacity of fine mineral particles into N saturation theory can improve predictions of N saturation rates and resolve inconsistent relationships between soil organic matter, texture, N mineralization, and N retention.

Key words: soil; texture; net; nitrification; particulate organic matter; nitrogen retention; gross nitrogen mineralization; gross nitrification.

INTRODUCTION

Soil nitrogen (N) mineralization can impact ecosystem processes including primary productivity

and nitrate leaching (Vitousek and others 1997). Ecosystem models typically include soil texture as one of several mechanistic controls on N mineralization (for example, Parton 1994). In these models, N mineralization and sand are positively correlated because silt and clay particles stabilize potentially mineralizable soil organic matter (SOM). However, empirical work has demonstrated that N mineralization and sand concentration can be positively, negatively or not correlated (for example, Reich and others 1997; Cote and others 2000; Giardina and others 2001; Bechtold

Received 18 July 2011; accepted 7 October 2011

Electronic supplementary material: The online version of this article (doi:10.1007/s10021-011-9501-3) contains supplementary material, which is available to authorized users.

Author Contributions: MJC and JPK analyzed the data and wrote the manuscript. MJC, JPK, HL, and JPS designed the study.

*Corresponding author; e-mail: castellanomichaelj@gmail.com

and Naiman 2006). Negative correlations between N mineralization and sand are often attributed to the tendency for sand to be negatively correlated with total SOM. This interpretation is based on the widespread positive correlation between SOM and N mineralization (Booth and others 2005).

These inconsistent relationships between soil texture and N mineralization can be reconciled by incorporating C saturation theory (Stewart and others 2007) into conceptual models of N retention and saturation (Vitousek and others 1997; Aber and others 1998). Carbon saturation theory is based on the capacity of silt and clay particles to physico-chemically stabilize C, protecting it from mineralization (Sollins and others 1996). Carbon saturation theory demonstrates that the capacity of silt and clay to stabilize C is limited; when the capacity of silt and clay to stabilize C becomes saturated, additional C inputs cannot be stabilized and remain available for rapid mineralization.

Because soil C and N concentrations are well correlated with strong biological links and consistent stoichiometry (Cleveland and Liptzin 2007), C saturation concepts should apply to N stabilization and mineralization. The absolute capacity of silt + clay to stabilize C and N is a positive linear function of silt + clay content (Hassink 1997). However, the proportion of new organic matter (OM) inputs that can be stabilized by the silt + clay fraction decreases in proportion to the amount of OM already present in the fraction. Accordingly, as the capacity for silt + clay to stabilize OM approaches zero (that is saturation), the efficiency of OM stabilization decreases and a greater proportion of OM inputs accumulate in the easily mineralizable particulate OM (POM) fraction (Stewart and others 2007).

These recent advances in C saturation theory combined with the tight coupling of C and N in SOM (Kaye and others 2002; Cleveland and Liptzin 2007; Stewart and others 2007) led us to develop a new conceptual model linking OM concentrations in the silt + clay mineral-associated OM (MAOM) soil fraction and N retention capacity (Figure 1). The premise of this model is that soil texture and OM inputs should interact to affect MAOM concentrations in the silt + clay fraction and thus the capacity for N retention and the rate of N saturation. When MAOM concentrations in the silt + clay fraction are low and far from saturation, N retention in MAOM is expected to be high. In this case, dissolved organic N (DON) compounds are rapidly adsorbed to silt + clay soil particles, inhibiting N mineralization. This mechanism also applies to the retention of inorganic N inputs in SOM,

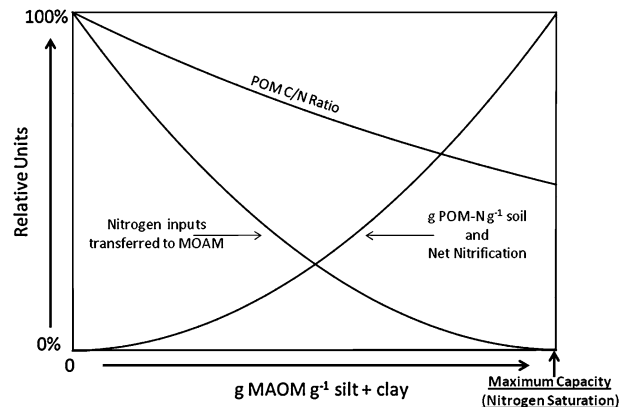


Figure 1. Responses of soil organic matter and nitrogen dynamics (y axis) to increasing concentrations of mineral associated organic matter (MAOM) nitrogen in the silt + clay soil fraction ($\text{g MAOM-N g silt + clay}^{-1}$; x axis). The absolute capacity for MAOM-N storage ($\text{g MAOM-N g soil}^{-1}$) is finite (Hassink 1997). However, as MAOM-N concentrations increase, the amount of N inputs transferred to MAOM are expected to decrease exponentially. Nitrogen inputs that are not transferred to MAOM should remain in actively cycled POM fractions. As POM accumulates, the C/N ratio of POM is expected to decrease due to carbon mineralization. Accordingly, microbial N demands are increasingly met and N mineralization increases. Although not indicated in this model, net nitrification could continue to increase after MAOM-N saturation as a result of continued N inputs, soil acidification, and vegetation mortality.

which occurs primarily through rapid microbial transformation of inorganic N to DON (Norton and Firestone 1996; Zogg and others 2000; Kaye and others 2002). However, as MAOM accumulates, MAOM concentrations in the silt + clay fraction will increase toward saturation and the efficiency of DON adsorption in MAOM should decrease. In response, N and C inputs that are not retained in stable MAOM pools will accumulate in the actively cycling labile POM fraction (Six and others 2002). As N and C concentrations in unprotected POM increase, gross N and C mineralization should increase, but POM C/N ratios should decrease because N mineralization is partially balanced by N immobilization (while mineralized C is lost from the soil system as CO_2). High gross N mineralization and lower POM C/N ratios should satisfy plant and heterotrophic N demand, leading to a final prediction, that net nitrification should increase with increasing MAOM concentrations on silt + clay particles.

To test our conceptual model, we measured OM fractions, gross and net ammonification and nitrification, and $^{15}\text{NH}_4\text{-N}$ transfer to SOM in A and B soil horizons across a 0.5 ha temperate forest.

The site was well suited for isolating the effect of MAOM on N cycling because it exhibits broad soil texture gradients, but other factors that may affect N cycling (climate, vegetation, and stand age) did not vary. Based on predictions of C saturation theory, we expected that MAOM concentrations in the silt + clay fraction would differ across particle size distributions and soil horizons due to differences in MAOM stabilization capacity (particle size variation) and OM inputs (horizons). Accordingly, our overarching hypothesis was that soil retention of added N would decrease and nitrification would increase as MAOM concentrations in the silt + clay fraction increase toward saturation.

METHODS

The approximately 0.5 ha study site is located in Abingdon, MD USA (39°27'05"N, 76°16'23"W). The site is part of the Chesapeake Bay, MD National Oceanic and Atmospheric Association National Estuarine Research Reserve. Mean annual temperature is 12.0°C. Mean annual precipitation is 1,164 mm. Vegetation at the site is a mix of *Liquidambar styraciflua*, *Liriodendron tulipifera*, and *Quercus* spp. Tree ring analyses indicate that many individuals of the dominant tree species (*L. styraciflua*) are more than 110 years old (unpublished data). Soils are all well drained and derived from alluvial Coastal Plain deposits. Two of three soil series at the site are Typic Hapludults (Joppa and Elsinboro series); the third is a Lamellic Quartzipsamment (Evesboro series). The site is part of a small catchment that spans upland to floodplain. The three soil series, soil texture gradient, and site drainage are all parallel, running from NE to SW. The NE end of the gradient contains the least sand (~50%) and the SW end of the gradient contains the most sand (>90%). We located eight sample locations in the upland, eight locations on the hill slope, and eight locations toward, but above, the floodplain ($n = 24$). Our soil samples did not exhibit redoximorphic features or alluvial discontinuities. In August 2008, we extracted five replicate A horizon cores at all 24 sample locations and five replicate B horizon soil cores at 16 of the 24 locations using a 15 cm deep \times 5 cm diameter soil core sampler and butyrate liners (that is, 200 soil cores sampled in butyrate liners). Sampling of B horizons at the eight locations at the bottom of the catena was prevented due to deep (>30 cm) B horizons that exhibited redoximorphic features. Soil from the 200 cores was used for all analyses. In a few locations, the A horizon was less than 15 cm deep; in these situations we removed the B horizon portion from the soil core prior to analyses.

Soil texture was determined with the method presented by Kettler and others (2001) on one composite sample derived from the five soil cores at each location. Bulk density was measured for each core using the mass of dry soil (<2 mm) and the volume of sample. Throughfall fluxes of $\text{NH}_4\text{-N} + \text{NO}_3\text{-N}$ measured at each A horizon sampling location in 2009 ranged from 4.5 to 9.1 kg ha⁻¹ with no discernable pattern across the site (unpublished data). pH was determined in a 1:1 (soil mass:deionized water volume) ratio.

On the August 2008 sampling date, using the five intact soil cores in butyrate liners, we measured in situ 3-day gross ammonification and nitrification with the isotope pool dilution method (Hart 1994). We selected a 3-day incubation time to insure sufficient NH_4 and NO_3 production in the relatively dry summer soils. At the inception of the in situ incubation immediately after soil core extraction, two cores were injected with $^{15}\text{NH}_4\text{Cl}$, two cores were injected with K^{15}NO_3 , and the fifth core was reserved to determine ^{15}N natural abundance. Soil cores from the A horizon were injected with 0.75 mg of 70.4% APE $^{15}\text{NH}_4\text{Cl-N}$ and 0.5 mg of 60.2% APE $\text{K}^{15}\text{NO}_3\text{-N}$ whereas B horizon soil cores were injected with 0.6 mg of 70.4% APE $^{15}\text{NH}_4\text{Cl-N}$ and 0.4 mg of 60.2% APE $\text{K}^{15}\text{NO}_3\text{-N}$. All N applications were delivered in injections of deionized water that totaled 5 ml of solution per soil core and increased soil moisture by approximately 1.7%. On average, these ^{15}N additions increased the A horizon NH_4 pool by 17%, the B horizon NH_4 pool by 26%, the A horizon NO_3 pool by 26%, and the B horizon NO_3 pool by 35%. Cores were capped at both ends; the top cap was perforated to allow for gas exchange. fifteen min after injection, the ambient core, one $^{15}\text{NH}_4\text{Cl}$ -injected soil core and one K^{15}NO_3 -injected soil core were extracted for NH_4 and NO_3 by reciprocal shaking for 2 h in a 2 M KCl solution at a m/v ratio of 1:5 (soil:KCl). After shaking, the solution was filtered (pre-leached Whatman 1) for determination of $\text{NH}_4\text{-N}$ and $\text{NO}_3\text{-N}$ on a flow injection spectrophotometer. The remaining $^{15}\text{NH}_4\text{Cl}$ -injected soil core and K^{15}NO_3 -injected soil core were left in the field to incubate for 3 days, and then extracted using the above procedure. We followed laboratory procedures and calculated gross N cycling rates as well as NH_4 and NO_3 consumption rates as presented in Hart (1994). Unlike isotope dilution estimates of gross mineralization, gross consumption rates are susceptible to overestimation due to substrate stimulation (Hart 1994). Solid sample C and N concentrations and N isotope ratios were determined at the University of California Stable Isotope

Facility (Davis, CA) with an elemental analyzer interfaced to an isotope ratio mass spectrometer. Total soil C and N are the means of the five soil core samples from each sample location. Isotope ratios of $\text{NH}_4\text{-N}$ and $\text{NO}_3\text{-N}$ were also determined by this procedure after diffusion of each species to acidified filter paper (Stark and Hart 1996). Using 2 mm sieved, air-dried soil from the ambient cores that were not amended with N, we conducted a 30-day potential net N mineralization analysis in the lab (Binkley and Hart 1989). We extracted one subsample for NH_4 and NO_3 with the above procedure at the onset of the incubation. A paired subsample was maintained at 60% water holding capacity and 20°C for 30 days and then extracted for NH_4 and NO_3 . The net change in NH_4 and NO_3 concentrations from 0 to 30 days were interpreted as potential net ammonification and nitrification.

Subsamples of 2 M KCl-extracted soil from the 3-day $^{15}\text{NH}_4\text{Cl}$ field incubations were physically fractionated into sand-associated POM and silt + clay MAOM (Moran 2006) so that we could determine the concentration of POM- and MAOM-associated C and N as well as the 15 min to 3-day transfer of NH_4 (via the 15 min $^{15}\text{NH}_4\text{Cl}$ label) to POM and MAOM insoluble organic N pools. The POM and MAOM- NH_4 sinks represent fractions of NH_4 consumption. We selected soils from the 3-day $^{15}\text{NH}_4\text{Cl}$ field incubations from the four ^{15}N additions because (1) time did not permit analysis of $^{15}\text{KNO}_3$ and $^{15}\text{NH}_4\text{Cl}$, (2) NH_4 is more rapidly transferred to SOM than NO_3 in our own preliminary data and in many other N retention studies, and (3) $^{15}\text{NH}_4$ transfer generally increases from minutes to days because it is biologically mediated (Fitzhugh and others 2003; Fricks and others 2009). For example, as a fraction of the ^{15}N -labeled $\text{NH}_4\text{-N}$ pool, 14% of $\text{NH}_4\text{-N}$ was transferred to insoluble OM at 15 min whereas 26% of $\text{NH}_4\text{-N}$ was transferred to insoluble OM on the third day. Moreover, NH_4 is the dominant soil inorganic N species at our site.

We physically fractionated soil samples after oven-drying at 65°C until a constant mass was achieved. After drying, 10 g of soil was dispersed in deionized water by reciprocal shaking for 16 h. After shaking, solutions were poured onto a 53- μm sieve placed above 1,500-ml Pyrex beaker. The sieve catches the greater than 53 μm POM + sand (POM fraction). DI water was used to rinse silt + clay and MAOM through the sieve until the water exiting the sieve was visibly clear against a white background. The silt + clay + MAOM + DI water were dried at 65°C until a constant mass was achieved. Greater than 98% soil recovery was achieved for all samples.

Dried samples were analyzed for total C, total N, and ^{15}N APE. The amount of $^{15}\text{NH}_4\text{-N}$ that was retained in MAOM and POM insoluble soil organic N fractions after the 3-day incubation was determined with two-pool mixing models. $^{15}\text{NH}_4\text{-N}$ that was not recovered in OM was determined by subtraction and includes ^{15}N tracer extracted in the KCl (organic and inorganic) or lost to gaseous species during the incubation (although significant denitrification was unlikely due to aerobic soil conditions).

We compared the amount of $^{15}\text{NH}_4\text{-N}$ transferred to POM and MAOM with three procedures. First, using the $^{15}\text{NH}_4\text{-N}$ tracer as a label for the NH_4 pool over the 3-day incubation, we compared the fraction of the total 15 min-extracted $\text{NH}_4\text{-N}$ pool that was transferred to POM and MAOM on the third day. We compared fractions because a different mass of $^{15}\text{NH}_4\text{-N}$ was added to A and B horizons to permit detection of the isotope while minimizing potential effects of the added NH_4 on N cycling. This measure provides a comparison of the efficiency of NH_4 transfer to POM and MAOM because NH_4 concentrations are chronically lower in B horizons (~50%) and vary across the texture and OM gradients at our site (unpublished data). Second, we calculated the absolute mass of $\text{NH}_4\text{-N}$ per mass of dry soil ($\text{NH}_4\text{-N}$ kg^{-1} dry soil) transferred to POM and MAOM pools between the 15 min and 3-day extractions. Third, we calculated the absolute mass of $\text{NH}_4\text{-N}$ per mass of MAOM-N ($\text{NH}_4\text{-N}$ kg^{-1} MAOM-N) transferred to POM and MAOM pools between the 15 min and 3-day extractions to isolate the effect of MAOM on N retention. Although we added 0.15 mg more to $\text{NH}_4\text{-N}$ to the A horizons, this difference represented a small fraction of total $\text{NH}_4\text{-N}$ pools (<10%) at the time of injection. All procedures assume that the initial NH_4 pool size and concentration at each sample location is identical in soil cores extracted at 15 min and 3 days. Similar to $\text{NH}_4\text{-N}$ transfer to insoluble OM pools (POM and MAOM), N mineralization rates were calculated per mass of dry soil (<2 mm) and per mass of MAOM-N.

Paired *t* tests of log10 transformed data were used to compare properties across soil horizons where A and B horizons were sampled (16 pairs). All variables were log10 transformed to facilitate comparison among homoscedastic and heteroscedastic variables. We analyzed data from all 40 samples for general positive and negative relationships with Pearson's correlation coefficient after log10 transformation because variables exhibited exponential and linear relationships as well as heteroscedasticity. However, for direct tests of our conceptual model (Figure 1), we analyzed data with univariate

linear and nonlinear exponential correlations; for these analyses, we only used log10 transformation when required to meet analytical assumptions. The model fit with the lowest total corrected sum of squares is reported and untransformed data are displayed. Dependent variables included POM concentrations in the total soil, POM C/N ratio, gross N mineralization, potential net N mineralization, and the transfer of $^{15}\text{NH}_4\text{-N}$ to POM and MAOM soil fractions after 3 days in situ field incubation. Independent variables included sand concentration, POM-C and N kg sand^{-1} , POM-C and N kg soil^{-1} , POM-C/N ratio, MAOM-C and N $\text{kg silt + clay}^{-1}$, MAOM-C and N kg soil^{-1} , and MAOM-C/N ratio. We sampled A and B soil horizons to maximize variation in soil properties so that we could identify widespread controls on N mineralization and retention. Therefore, we focused analyses on soil properties that continuously scaled N cycling processes across both horizons. Our sample sizes (40) coupled with the large number of independent variables precluded the use of multiple regression due to a loss of statistical power. We report the probability of type I error to 0.00005 due to the number of independent statistical analyses.

RESULTS

Soil Properties and Scalars of Nitrogen Dynamics

Sand concentrations ranged from 490 to 940 g kg^{-1} soil and C/N ratios ranged from 15 to 26 (Table 1). Across the 24 A horizon and 16 B horizon samples ($N = 40$), total soil C and N were well correlated ($R = 0.98$, $P < 0.0001$) as were MAOM-C and MAOM-N ($R = 0.98$, $P < 0.0001$) and POM-C and POM-N concentrations ($R = 0.98$, $P < 0.0001$). Therefore, we report all data in relationship to N rather than C because N is the focus of this paper. Bulk density was not correlated with sand; therefore, we report all N cycling processes as a mass of N kg^{-1} soil (particles < 2 mm).

Gross and net ammonification and nitrification rates, when calculated per mass of MAOM-N (mg N kg^{-1} MAOM-N), were not correlated with soil properties. However, gross and net ammonification and nitrification rates, when calculated per mass of soil, were correlated with many soil properties (Online Appendix); thus, we report gross and net ammonification and nitrification rates per mass of soil rather than MAOM-N. In contrast to gross and net ammonification and nitrification rates, $\text{NH}_4\text{-N}$ transferred to insoluble POM and MAOM pools at the end of the 3-day incubation was

correlated with soil properties when calculated as: (1) a fraction of the total $\text{NH}_4\text{-N}$ pool extracted at 15 min; (2) the absolute mass of the $\text{NH}_4\text{-N}$ pool extracted at 15 min per kg of dry soil; and (3) the absolute mass of the $\text{NH}_4\text{-N}$ pool extracted at 15 min per kg of MAOM-N.

Paired Comparisons of Soil Horizons

Paired t test comparisons between horizons ($N = 16$) demonstrated that sand, silt, and clay concentrations did not differ between the A and B horizons. However, concentrations of total N, POM-N, and MAOM-N were all higher in the A horizon (Table 1). Similarly, gross and net ammonification and nitrification as well as gross NH_4 consumption rates were higher in the A horizon (Table 1).

A smaller fraction of $\text{NH}_4\text{-N}$ was transferred to A horizon MAOM compared to B horizon MAOM (Table 1), but the absolute mass of $\text{NH}_4\text{-N}$ transferred to MAOM ($\text{mg NH}_4\text{-N}$ transferred to MAOM kg^{-1} soil) did not differ between horizons. In contrast, the fraction of $\text{NH}_4\text{-N}$ that was transferred to POM did not differ across horizons, but a larger absolute mass of $\text{NH}_4\text{-N}$ was transferred to A horizon POM ($\text{mg NH}_4\text{-N kg}^{-1}$ soil; Table 1). In both A and B horizons, a larger fraction and absolute mass of $\text{NH}_4\text{-N}$ was transferred to MAOM than POM (Table 1).

Nitrogen Dynamics Across Soil Horizons

Sand concentrations were not correlated with total N or C/N ratios (Online Appendix). However, sand concentrations were positively correlated with MAOM-N concentrations in the silt + clay fraction (although the slope of this relationship differed between horizons; Figure 2A). Concentrations of MAOM-N in the silt + clay fraction were positively correlated with concentrations of POM-N in the total soil (Figure 2B) and negatively correlated with POM C/N ratios (although the slope of this relationship differed between horizons; Figure 2C).

Across soil horizons, total soil N, POM-N, and MAOM-N were well correlated with gross and net ammonification and nitrification rates (Figure 3; Online Appendix). In contrast, correlations between sand, C/N ratios and gross and net ammonification and nitrification rates were relatively poor (Online Appendix). Within-horizon correlations between sand, C/N ratios and gross and net ammonification and nitrification rates were poor when compared to across horizon correlations between total soil N, POM-N, MAOM-N, and gross

Table 1. Soil Properties

Soil properties	Paired A and B horizon locations						Unpaired A horizon locations		
	A horizon			B horizon			A horizon		
	Minimum	Maximum	Mean	Minimum	Maximum	Mean	Minimum	Maximum	Mean
Sand (g kg ⁻¹)	530	940	700	490	920	700	670	930	770
Silt (g kg ⁻¹)	10	370	210	40	370	200	10	220	150
Clay (g kg ⁻¹)	30	160	90	40	140	100	60	110	80
Bulk density (g cm ⁻³)	0.58	1.11	0.83	0.66	1.56	1.08	0.48	0.99	1.00
pH	3.10	3.90	3.70	3.20	4.70	4.00	3.30	4.30	3.90
Total organic nitrogen (g kg ⁻¹)	0.89	2.82	1.58	0.22	0.81	0.43	1.50	2.88	2.18
C/N ratio	18.20	25.90	20.80	15.10	22.20	17.40	20.20	26.10	22.40
POM-N (g kg ⁻¹ sand)	0.20	2.04	0.89	0.04	0.55	0.17	0.27	3.43	1.36
POM-N (g kg ⁻¹ soil)	0.13	1.87	0.64	0.03	0.46	0.12	0.0001	1.59	0.83
POM C/N	21.69	39.97	28.40	21.46	40.32	29.34	0.8177	33.47	28.45
MAOM-N (g kg ⁻¹ silt + clay)	1.42	9.80	4.14	0.61	3.69	1.73	<0.0001	8.54	5.11
MAOM-N (g kg ⁻¹ soil)	0.59	1.77	1.03	0.17	0.69	0.45	<0.0001	1.50	1.05
MAOM-C/N	14.57	22.32	17.06	7.58	18.55	13.88	<0.0001	26.00	18.59
Gross ammonification (mg kg ⁻¹ soil day ⁻¹)	0.21	3.56	1.30	0.03	1.27	0.64	0.0074	3.68	1.79
Gross nitrification (mg kg ⁻¹ soil day ⁻¹)	0.11	0.98	0.39	0.08	0.32	0.16	0.0019	0.45	0.34
Gross NH ₄ consumption (mg kg ⁻¹ soil day ⁻¹)	0.60	5.41	2.37	0.00	3.37	1.26	0.0065	4.96	3.10
Gross NO ₃ consumption (mg kg ⁻¹ soil day ⁻¹)	-0.20	0.96	0.25	-0.11	0.66	0.16	0.5296	0.74	0.32
Net ammonification (mg kg ⁻¹ soil day ⁻¹) ¹	0.54	1.98	1.23	0.07	0.46	0.23	<0.0001	2.38	1.32
Net nitrification (mg kg ⁻¹ soil day ⁻¹) ¹	0.71	1.42	1.09	0.04	0.51	0.25	<0.0001	1.32	1.09
NH ₄ transfer to POM (%) ²	1.25	8.93	4.95	0.81	7.92	4.01	0.2217	9.66	4.69
NH ₄ transfer to MAOM (%) ²	8.16	24.17	16.66	13.22	51.00	29.84	<0.0001	21.82	12.87
NH ₄ unrecovered (%) ²	67.84	87.40	78.39	45.32	81.63	66.15	<0.0001	86.65	82.44
NH ₄ transfer to POM (mg kg ⁻¹ soil) ³	0.04	0.33	0.19	0.03	0.19	0.09	0.0001	0.50	0.23
NH ₄ transfer to MAOM (mg kg ⁻¹ soil) ³	0.35	0.90	0.64	0.37	1.35	0.67	0.5935	0.82	0.57
NH ₄ unrecovered (mg kg ⁻¹ soil) ³	1.76	6.16	3.21	0.06	2.64	1.50	<0.0001	5.13	3.87
NH ₄ -N transfer to POM (g kg ⁻¹ MAOM-N) ⁴	0.07	0.32	0.19	0.08	0.64	0.23	0.3671	0.35	0.23
NH ₄ -N transfer to MAOM (g kg ⁻¹ MAOM-N) ⁴	0.33	1.27	0.66	0.63	4.64	1.74	<0.0001	1.40	0.67
NH ₄ -N unrecovered (g kg ⁻¹ MAOM-N) ⁴	1.95	6.26	3.25	0.13	13.16	4.09	0.3241	8.42	4.17

¹Calculated as the net change in NH₄-N or NO₃-N pools after a 30-day laboratory incubation.²Calculated as a proportion of the total salt-extracted NH₄-N pool measured 15 min after ¹⁵NH₄-N addition that was transferred or unrecovered after the 3-day incubation.³Calculated as the total mass of the salt-extracted NH₄-N pool measured 15 min after ¹⁵NH₄-N addition that was transferred or unrecovered after the 3-day incubation.⁴Calculated as the total mass of the salt-extracted NH₄-N pool measured 15 min after ¹⁵NH₄-N addition that was transferred or unrecovered after the 3-day incubation.

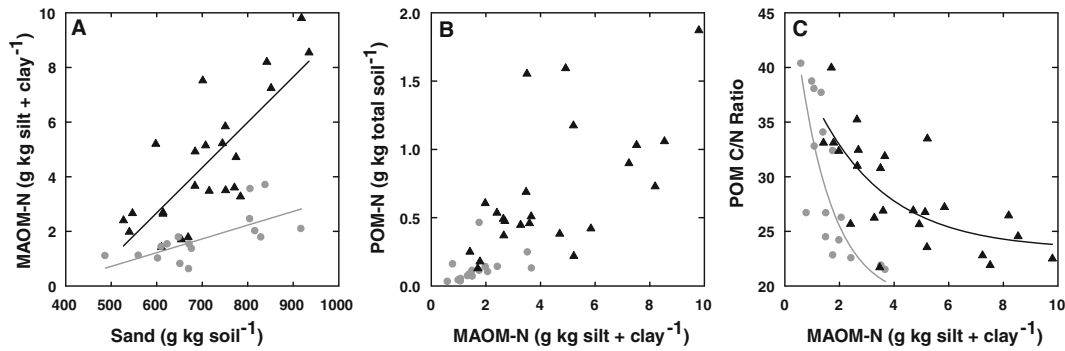


Figure 2. Black triangles indicate A horizon samples and gray circles indicate B horizon samples. Solid lines indicate the model fit. **A** Sand concentration and mineral-associated organic matter nitrogen concentration in the silt + clay soil fraction (MAOM-N) were positively correlated within soil horizons. For the A horizon $y = 0.02x - 7.28$; $R = 0.78$, $P < 0.0001$ and for the B horizon $y = 0.01x - 1.8$, $R = 0.68$, $P = 0.0034$. **B** MAOM-N concentration in the silt + clay soil fraction was positively correlated with particulate organic matter N (POM-N) in the total soil ($\text{Log}(y) = 1.34\text{log}x + -1.13$, $R = 0.81$, $P < 0.0001$). Data were log_{10} transformed prior to analysis to correct for heteroscedasticity, thus, no regression line is displayed. **C** MAOM-N concentration in the silt + clay soil fraction was negatively correlated with POM C/N ratio within horizons. For the A horizon $y = 23.33 + 20.65e^{(-0.38x)}$; $R = 0.72$; $P = 0.0005$. For the B horizon $y = 18.57 + 33.49e^{(-0.79x)}$; $R = 0.68$; $P = 0.0165$.

and net ammonification and nitrification rates (Online Appendix). Gross NH_4 consumption was positively correlated with total soil N, POM-N and MAOM-N. However, gross NO_3 consumption was not correlated with soil properties (Online Appendix).

The fraction of NH_4 -N that was transferred to insoluble MAOM during the 3-day in situ incubation was negatively correlated with sand, total N, MAOM-N, and POM-N (Figure 4A; Online Appendix). These relationships were all similar and best fit by exponential decay equations. Of these relationships, the fraction of NH_4 -N transferred to MAOM was most closely correlated with MAOM-N concentrations in silt + clay (Figure 4A). In contrast, the fraction of NH_4 -N that was retained in insoluble POM after the 3-day in situ incubation was positively related to POM-N in the total soil and this relationship was best fit by an exponential rise to maximum equation (Figure 4B). The fraction of NH_4 -N that was not recovered in insoluble OM (POM or MAOM) was positively correlated with sand, total N, POM-N, and MAOM-N. These relationships were all best fit by an exponential rise to maximum equation. Of these relationships, the fraction of NH_4 -N that was not recovered in insoluble OM was most closely correlated with MAOM-N concentrations in the silt + clay fraction (Figure 4C). In comparison to the fraction of NH_4 -N transferred to OM, relationships between the absolute mass of NH_4 -N that was transferred to, or not recovered in OM were similar and significant but not as strong (Online Appendix).

The absolute mass of NH_4 -N transferred to insoluble MAOM calculated per mass of MAOM-N ($\text{g NH}_4\text{-N transferred to MAOM kg}^{-1}$ MAOM-N), was negatively correlated with total N, POM-N, and MAOM-N (Online Appendix). These relationships were similar and best fit by an exponential decay equation. The mass of NH_4 -N transferred to POM and the mass of NH_4 -N that was not recovered in insoluble OM (kg^{-1} MAOM-N) were relatively poorly correlated with soil properties (Online Appendix).

Gross and net ammonification and nitrification rates were negatively correlated with the fraction of NH_4 -N transferred to MAOM but positively correlated with the fraction and absolute mass of NH_4 -N that was not recovered in POM or MAOM ($\text{mg NH}_4\text{-N unrecovered in POM or MAOM kg}^{-1}$ soil; Figure 5; Online Appendix). Gross and net ammonification and nitrification rates were positively correlated with the absolute mass of NH_4 -N transferred to POM ($\text{mg NH}_4\text{-N transferred to POM kg}^{-1}$ soil; Online Appendix). Gross and net ammonification and nitrification rates were negatively correlated with the absolute mass of NH_4 -N that was transferred to MAOM ($\text{mg NH}_4\text{-N in MAOM kg}^{-1}$ MAOM-N). These relationships were best fit by exponential decay equations (Online Appendix).

DISCUSSION

Data from this site suggest that concentrations of MAOM on silt and clay particles affect N mineralization and retention. Transfer of NH_4 -N to insoluble

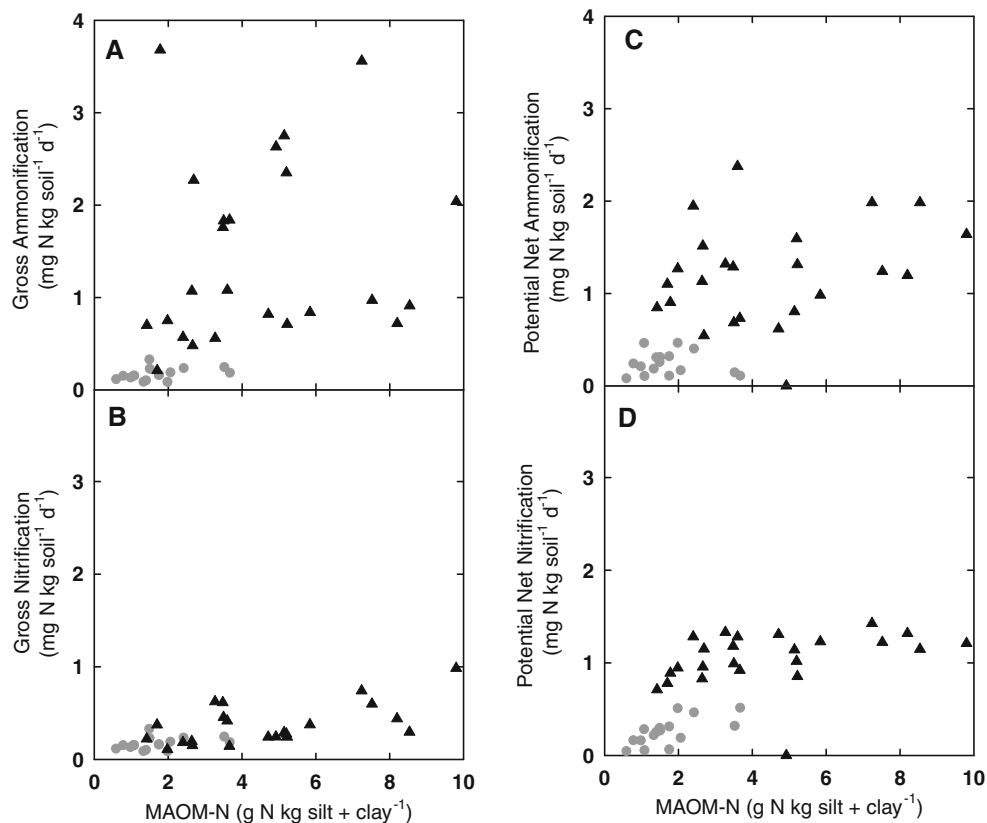


Figure 3. Across both soil horizons, gross and net ammonification and nitrification rates were positively correlated with mineral-associated organic matter nitrogen (MAOM-N) concentrations in the silt + clay fraction: **A** $\text{Log}(y) = 0.89\text{-log}(x) + -0.48$; $R = 0.63$, $P < 0.0001$. **B** $\text{Log}(y) = 0.62 \text{ log}(x) + -0.90$; $R = 0.70$, $P < 0.0001$. **C** $\text{Log}(y) = 0.92\text{-log}(x) + 0.84$; $R = 0.64$, $P < 0.0001$. **D** $\text{Log}(y) = 1.09\text{log}(x) + 0.74$; $R = 0.76$, $P < 0.0001$. Data were log10 transformed prior to analysis to meet analytical assumptions. Original data are displayed; thus, models are not shown. *Black triangles* indicate A horizon samples and *gray circles* indicate B horizon samples.

MAOM was negatively correlated with MAOM concentrations in silt + clay (Figure 4; Online Appendix) whereas gross and net ammonification and nitrification were positively correlated with MAOM concentrations in silt + clay (Figure 3). Moreover, the transfer of $\text{NH}_4\text{-N}$ to MAOM was negatively correlated with gross and net ammonification and nitrification (Figure 5; Online Appendix). Across the texture and SOM gradients at our site, POM, MAOM, and total N were consistently better correlated with N dynamics than texture or C/N ratios (Figures 3, 4, 5; Online Appendix).

Conceptual Model Evaluation

Our conceptual model for N retention and mineralization is based on the capacity of fine soil particles to physico-chemically stabilize C and N inputs. The capacity of fine soil particles to stabilize OM is affected by particle size and the cumulative amount of OM inputs (Hassink 1997; Stewart and others

2007). Using a particle size gradient and soil horizons, we maximized variation in OM stabilization capacity and inputs to provide an initial test of our model (Table 1; Figure 1), and several key predictions were supported. Concentrations of MAOM in the silt + clay particle fraction and concentrations of POM in the total soil were positively correlated (Figure 2B). This pattern is consistent with C saturation principles that suggest increasing MAOM-C concentrations in fine particles will lead to an accumulation of POM-C and an increase in C mineralization (Stewart and others 2007; Gulde and others 2007). Our data extend this relationship to N by demonstrating that increasing MAOM concentrations are also coincident with an increase in POM-N and a decrease in POM C/N ratios (Figure 2C). Based on C saturation theory and these data, increasing MAOM concentrations should also increase N mineralization. Indeed, N mineralization was positively correlated with MAOM (Figure 3).

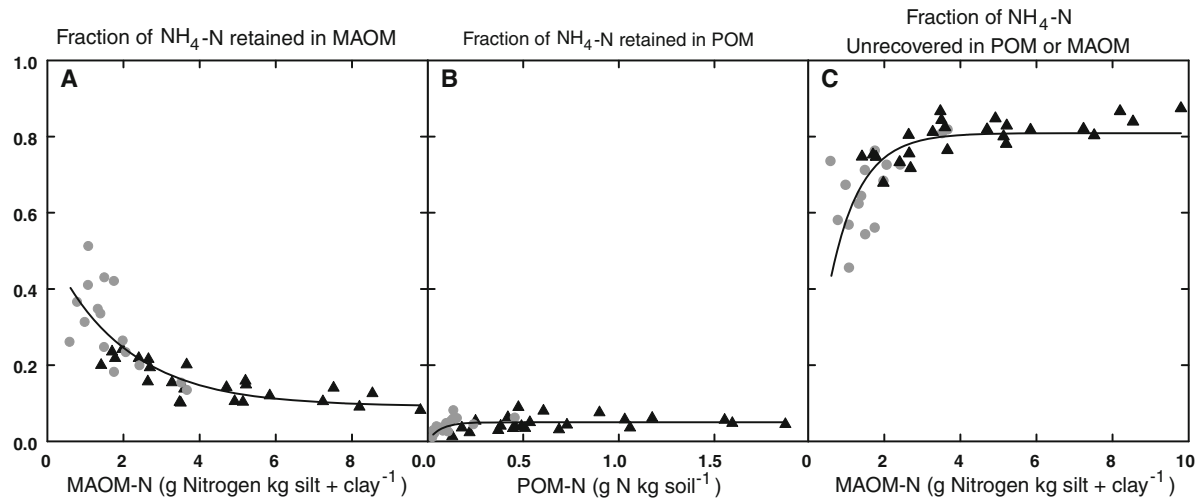


Figure 4. Across both horizons, the fraction of the initial $\text{NH}_4\text{-N}$ pool that was transferred to insoluble organic matter or not recovered in insoluble organic matter during a 3-day in situ incubation: **A** The fraction of $\text{NH}_4\text{-N}$ transferred to insoluble silt + clay mineral associated organic matter (MAOM) was most closely correlated with MAOM-nitrogen (MAOM-N) concentrations in silt + clay ($y = 0.09 + 0.42e^{(-0.51x)}$; $R = 0.82$; $P < 0.0001$). **B** The fraction of $\text{NH}_4\text{-N}$ transferred to insoluble POM was most closely correlated with POM nitrogen (POM-N) concentrations in the total soil ($y = 0.05(1 - e^{(-15.15x)})$; $R = 0.50$, $P = 0.0010$). **C** The fraction of $\text{NH}_4\text{-N}$ unrecovered in insoluble organic matter (POM or MAOM) was most closely correlated with MAOM-N concentrations in silt + clay $y = 0.81(1 - e^{(-1.26x)})$; $R = 0.65$, $P < 0.0001$). Solid lines indicate model fits. Fractions displayed across the three panels sum to 1.0. Black triangles indicate A horizon samples and gray circles indicate B horizon samples.

The positive correlations between gross and net ammonification and nitrification and MAOM (Figure 3) suggest that retention of N inputs in MAOM decreases with increasing MAOM concentrations in the silt + clay fraction. We explicitly examined this process by measuring $^{15}\text{NH}_4\text{-N}$ transfer to insoluble MAOM during a 3-day in situ incubation (Figures 4, 5; Online Appendix). Negative correlations between $^{15}\text{NH}_4\text{-N}$ transfer to MAOM (by fraction and mass) and concentrations of MAOM in silt + clay implicate a direct effect of MAOM concentrations on N retention (Figure 4; Online Appendix). In fact, the fraction of $^{15}\text{NH}_4\text{-N}$ transfer to MAOM and the absolute mass of $^{15}\text{NH}_4\text{-N}$ transfer to MAOM per kg of soil were also negatively correlated with concentrations of MAOM in the total soil (Online Appendix). Similar, but more variable, negative exponential relationships between $\text{NH}_4\text{-N}$ transfer to SOM and total N have been observed (Johnson and others 2000).

The ability of a soil to rapidly immobilize mineral N inputs into insoluble OM appears to be an important control on gross and net ammonification and nitrification rates. We observed gross and net nitrification to be negatively correlated with $^{15}\text{NH}_4\text{-N}$ transfer to MAOM and positively correlated with $^{15}\text{NH}_4\text{-N}$ that was not transferred to insoluble OM (Figure 5; Online Appendix). Our data are consis-

tent with research that demonstrates ecosystems with high N retention capacity typically have low nitrification whereas ecosystems with low N retention capacity typically have high nitrification (Emmett and others 1998). Our data advance large scale across-ecosystem research by demonstrating: (1) how N mineralization-immobilization processes can be affected by biophysical soil properties and (2) significant variation in these processes can occur at a relatively small scale within vegetation communities and N deposition amounts.

In contrast to our conceptual model predictions (Figure 1), increases in POM concentrations and gross and net ammonification and nitrification rates were linearly, rather than exponentially, correlated with concentrations of MAOM in silt + clay (Figures 2B, 3). These data are inconsistent with soil carbon saturation theory that suggests POM-C concentrations increase exponentially with increasing MAOM concentrations in silt + clay (Stewart and others 2007). However, small portions of exponential relationships can appear linear. It is possible that the range of MAOM concentrations in our experiment was not sufficient to observe the broader relationships between these variables. Figure 2A indicates that silt + clay particles at our site were not saturated with MAOM (C-saturated) because the increase in MAOM with

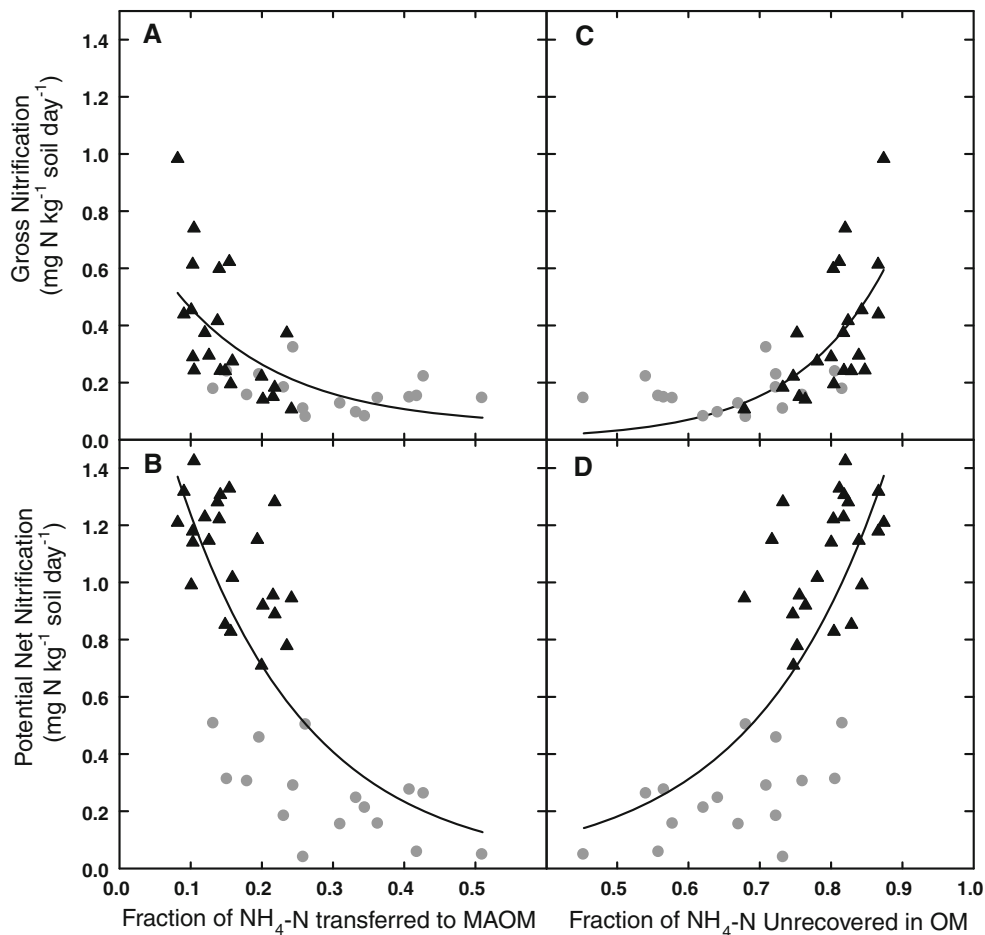


Figure 5. The fraction of $\text{NH}_4\text{-N}$ that was retained in insoluble mineral associated organic matter (MAOM) during a 3-day in situ incubation was negatively correlated with gross nitrification (**A**) $y = 1.11e^{(-7.95x)}$; $R = 0.69$; $P < 0.0001$ and potential net nitrification (**B**) $y = 2.16e^{(-5.55x)}$; $R = 0.78$; $P < 0.0001$. The fraction of $\text{NH}_4\text{-N}$ that was not recovered in insoluble POM or MAOM was positively correlated with gross nitrification (**C**) $y = 0.01e^{(7.80x)}$; $R = 0.69$; $P < 0.0001$ and potential net nitrification (**D**) $y = 0.01e^{(5.41x)}$; $R = 0.74$; $P < 0.0001$. Solid lines indicate model fit, Black triangles indicate A horizon samples, and gray circles indicate B horizon samples.

sand was linear rather than asymptotic at a maximum mass of MAOM-N kg^{-1} silt + clay (Stewart and others 2007). Nevertheless, the fraction of $\text{NH}_4\text{-N}$ transferred to MAOM-N appears to reach a minimum asymptote at around 10% (Figure 4A). These data may suggest MAOM-N concentrations in the silt + clay fraction are approaching saturation because the rate of N transfer to MAOM should decrease at an increasingly slower pace as MAOM accumulates (Figure 1; Stewart and others 2007). The rate of exponential decline in N transfer to MAOM in our conceptual model may be too shallow (Figure 1).

The accumulation of MAOM-N primarily occurs through sorption of DON compounds to silt and clay particles (Sollins and others 1996). Although the transfer of $\text{NH}_4\text{-N}$ to insoluble OM could differ from sorption of DON, laboratory and field research indicate that biotic processes dominate $\text{NH}_4\text{-N}$ transfer to insoluble OM through microbial transformation of $\text{NH}_4\text{-N}$ to DON (Norton and Firestone 1996; Barrett and Burke 2000; Fitzhugh and others 2003). Accordingly, microbial transformation of

$\text{NH}_4\text{-N}$ to DON and subsequent sorption to silt and clay particles was likely the dominant mechanism affecting $\text{NH}_4\text{-N}$ transfer to OM at our site. In fact, recent chemical characterization of SOM indicates stable MAOM pools may be disproportionately comprised of microbial-derived N compounds (Grandy and Neff 2008).

Nevertheless, abiotic mechanisms of $\text{NH}_4\text{-N}$ transfer to insoluble OM are included in our measurements. It is uncertain if abiotic N retention will follow our conceptual model. Some evidence suggests abiotic N retention may not be affected by soil N status (Johnson and others 2000). However, reports of greater total inorganic N immobilization in paired sterilized versus live soil laboratory incubations suggest microbes effectively compete with abiotic N sinks (Fitzhugh and others 2003; Fricks and others 2009; Lewis 2011). Therefore, some relationship between soil N status (microbial N demand) and abiotic N retention could be expected. Mineralogy is also an important soil property affecting DON sorption (Kaiser and Zech 2000) although we did not explore these relationships.

Soil Texture and Nitrogen Saturation Theory

Current N retention conceptual models do not explicitly include the capacity for silt + clay particles to stabilize mineral N inputs. However, empirical evidence demonstrates that ecosystems differ in absolute capacity for N retention and the rate of N saturation (Aber and others 1998; Emmett and others 1998; Magill and others 2000). For example, a 90-year-old forest on sandy soils within the Michigan Gradient study exhibited N saturation symptoms immediately after N additions ($30 \text{ kg NO}_3\text{-N ha}^{-1} \text{ y}^{-1}$; Pregitzer and others 2004). In contrast 50- and 70-year-old forests at the Harvard Forest exhibited relatively few symptoms of N saturation after 9 years of N additions ($50 \text{ kg NH}_4\text{NO}_3\text{-N ha}^{-1} \text{ y}^{-1}$; Magill and others 2000). Initial MAOM concentrations in the silt + clay soil fraction could partially explain the differences in the absolute capacity for N retention and the rate at which different ecosystems experience N saturation, especially after N additions (Figure 1).

Our conceptual model and results complement another recent conceptual model of N saturation that distinguishes between “capacity” N saturation, which occurs when N sinks are zero, and “kinetic” N saturation, which occurs when N input rates exceed sink strength (Lovett and Goodale 2011). Relative C saturation ($\text{MAOM}/\text{MAOM}_{\text{Maximum}}$) should be considered as a potential factor affecting N sink strength and this sink could be particularly strong in the subsoil. Indeed, concentrations of MAOM can affect capacity and kinetic N saturation processes. Soil texture can affect capacity N saturation whereas MAOM concentrations in silt + clay can affect kinetic N saturation. Soils with high silt + clay contents should have high N retention capacity; soils with low MAOM concentrations in the silt + clay fraction should have the ability to rapidly immobilize large amounts of N. However, the maximum rate of N immobilization should decrease exponentially as MAOM accumulates (Figures 1, 4A).

Based on these N retention processes and sinks, our conceptual model (Figure 1) can reconcile inconsistent relationships between soil texture and N mineralization. Positive relationships between sand and N mineralization may be due to MAOM saturation in sandy soils. In contrast, negative relationships between sand and N mineralization may be limited to soils with low MAOM concentrations in silt + clay (Figure 1). In such soils with a large saturation deficit, the proportion of OM inputs that are stabilized in MAOM would be very

high regardless of texture differences (Figures 1, 4; Stewart and others 2007). In these situations when N stabilization is close to 100% efficient, properties that are positively associated with N cycling and silt + clay (for example, water content) might be more important factors affecting N cycling than texture.

The Role of Subsoils

Conventional scalars of N mineralization and retention, including C/N ratios and total organic C (Lovett and others 2002; Booth and others 2005), could not characterize the wide range of gross and net ammonification and nitrification rates across surface and subsoils at our site (Online Appendix). In contrast, the full range of gross and net ammonification and nitrification rates observed at our site was scaled across both horizons by individual OM fractions (Figure 3). Total organic C is often positively correlated with N retention in A horizons due to high microbial activity and biomass (Nadelhoffer and others 1999; Barrett and others 2002; Booth and others 2005). However, at our site, B horizons with low total organic C retained a similar absolute mass of $^{15}\text{NH}_4\text{-N}$ as C-rich A horizon soils, and a larger fraction of $^{15}\text{NH}_4\text{-N}$ in MAOM (Table 1; Figure 4). These results build on a growing body of research that demonstrates subsoils can provide a significant mineral N sink (for example, Idol and others 2003; Dittman and others 2007). As OM and mineral N inputs are greatest in surface soils, our data suggest that subsoils will become progressively more important N sinks as surface soil silt + clay fractions accumulate N. Consistent with pedogenic development, the capacity of soils to stabilize OM should initially saturate in surface soils; afterward, saturation would be expected to progress downward through the soil profile.

Conclusions

By demonstrating that the capacity for silt + clay soil fractions to stabilize mineral $\text{NH}_4\text{-N}$ inputs is similar to the capacity of silt + clay fractions to stabilize organic C inputs (Figure 4), we extend C saturation theory to mineral N and link it with N retention and saturation theories. As the global N cycle accelerates, the capacity for ecosystems to retain N inputs will become an increasingly important ecosystem service. Across a wide array of sites, research shows that soils are the dominant sink for N inputs. However, there is substantial variation among sites. Our research leads to a new interpretation of that variation—soil texture,

through its influence on the capacity to stabilize OM, can explain a large fraction of variation in soil N retention. A mechanistic understanding of soil textural controls on N saturation complements prior models emphasizing N input levels, vegetation type, and microbial turnover (Aber and others 1998; Lovett and others 2004; Lovett and Goodale 2011). The relative importance of soil texture and MAOM controls on N retention will be maximized when other ecosystem properties that affect N dynamics, such as vegetation and N inputs, are similar (Lovett and others 2004). Nevertheless, the fundamental relationship between MAOM concentrations in the silt + clay fraction and N retention that operated across our within-site texture gradient could operate under the same mechanisms to explain across site variation. Nitrogen addition studies can be exploited to test the broad applicability of our results; sites with little or no capacity for OM stabilization in the silt + clay soil fraction would be expected to exhibit N saturation symptoms.

ACKNOWLEDGMENTS

Discussions with David Lewis improved the design of this experiment. This project was funded by NSF (DEB Dissertation Improvement Grant-090999) and NOAA (National Estuarine Research Reserve) to MJC. JPK was funded by NSF DEB 0816668. MJC was funded by USDA (National Needs 2005-38420-15774) to HL.

REFERENCES

Aber J, McDowell W, Nadelhoffer K, Magill A, Berntson G, Kamakea M, McNulty S, Currie W, Rustad L, Fernandez I. 1998. Nitrogen saturation in temperate ecosystems. *Bioscience* 48:921–34.

Barrett JE, Burke IC. 2000. Potential nitrogen immobilization in grassland soils across a soil organic matter gradient. *Soil Biol Biochem* 32:1707–16.

Barrett JE, Johnson DW, Burke IC. 2002. Abiotic nitrogen uptake in semiarid grasslands of the U.S. Great Plains. *Soil Sci Soc Am J* 66:979–87.

Bechtold JS, Naiman RJ. 2006. Soil texture and nitrogen mineralization potential across a riparian toposequence in a semi-arid savanna. *Soil Biol Biochem* 38:1325–33.

Binkley D, Hart S. 1989. The components of nitrogen availability assessments in forest soils. *Adv Soil Sci* 10:57–116.

Booth MS, Stark JM, Rastetter E. 2005. Controls on nitrogen cycling in terrestrial ecosystems: a synthetic analysis of literature data. *Ecol Monogr* 75:139–57.

Cleveland CC, Liptzin D. 2007. C:N:P stoichiometry in soil: is there a “Redfield ratio” for the microbial biomass? *Biogeochemistry* 85:235–52.

Cote L, Brown S, Pare D, Fyles J, Balthus J. 2000. Dynamics of carbon and nitrogen mineralization in relation to stand type,

stand age and soil texture in the boreal mixedwood. *Soil Biol Biochem* 32:1079–90.

Dittman JA, Driscoll CT, Groffman PM, Fahey TJ. 2007. Dynamics of nitrogen and dissolved organic carbon at the Hubbard Brook experimental forest. *Ecology* 88:1153–66.

Emmett BA, Boxman D, Bredemeier M, Gundersen P, Kjonaas OJ, Moldan F, Schleppe P, Tietema A, Wright RF. 1998. Predicting the effects of atmospheric nitrogen deposition in conifer stands: evidence from the NITREX ecosystem-scale experiments. *Ecosystems* 1:352–60.

Fitzhugh RD, Lovett GM, Venterea RT. 2003. Biotic and abiotic immobilization of ammonium, nitrite, and nitrate in soils developed under different tree species in the Catskill Mountains, New York, USA. *Glob Change Biol* 9:1591–601.

Fricks B, Kaye J, Seidel R. 2009. Abiotic nitrate retention in agroecosystems and a forest soil. *Soil Sci Soc Am J* 73:1137–41.

Giardina CP, Ryan MG, Hubbard RM, Binkley D. 2001. Tree species and soil textural controls on carbon and nitrogen mineralization rates. *Soil Sci Soc Am J* 65:1272–9.

Grandy AS, Neff JC. 2008. Molecular C dynamics downstream: the biochemical decomposition sequence and its impact on soil organic matter structure and function. *Sci Total Environ* 404:197–307.

Gulde S, Chung H, Amelung W, Change C, Six J. 2007. Soil carbon saturation controls labile and stable carbon pool dynamics. *Soil Sci Soc Am J* 72:605–12.

Hart SC, Stark JM, Davidson EA, Firestone MK. 1994. Nitrogen mineralization, immobilization, and nitrification. In: *Methods of Soil Analysis, Part 2—microbiological and biochemical properties*. Madison (WI): SSSA Book Series, no. 5. pp 985–1018.

Hassink J. 1997. The capacity of soils to preserve organic C and N by their association with clay and silt particles. *Plant Soil* 191:77–87.

Idol TW, Pope PE, Ponder F. 2003. N mineralization and N uptake across a 100-year old chronosequence of upland hardwood forests. *Forest Ecol Manag* 176:509–18.

Johnson DW, Cheng W, Burke IC. 2000. Biotic and abiotic nitrogen retention in a variety of forest soils. *Soil Sci Soc Am J* 64:1503–14.

Kaiser K, Zech W. 2000. Sorption of dissolved organic nitrogen by acid subsoil horizons and individual mineral phases. *Eur J Soil Sci* 51:403–11.

Kaye JP, Barrett JE, Burke IC. 2002. Stable carbon and nitrogen pools in grassland soils of variable texture and carbon content. *Ecosystems* 5:461–71.

Kettler TA, Doran JW, Gilbert TL. 2001. Simplified method for soil particle-size determination to accompany soil-quality analyses. *Soil Sci Soc Am J* 65:849–52.

Lewis DB, JP Kaye. 2011. Inorganic nitrogen immobilization in live and sterile soil of old-growth conifer and hardwood forests: implications for ecosystem nitrogen retention. *Biogeochemistry*. doi:10.1007/s10533-011-9627-6.

Lovett GM, Weathers KC, Arthur MA. 2002. Control of nitrogen loss from forested watersheds by soil carbon:nitrogen ratio and tree species composition. *Ecosystems* 5:712–18.

Lovett GM, Weathers KC, Arthur MA, Schultz JC. 2004. Nitrogen cycling in a northern hardwood forest: Do species matter? *Biogeochemistry* 67:289–308.

Lovett GM, Goodale CL. 2011. A new conceptual model of nitrogen saturation based on experimental nitrogen addition to an oak forest. *Ecosystems* 14:615–31.

- Magill AH, Aber JD, Bernston GM, McDowell WH, Nadelhoffer KJ, Melillo JM, Steudler P. 2000. Long-term nitrogen additions and nitrogen saturation in two temperate forests. *Ecosystems* 3:238–53.
- Moran KK, Jastrow J, O'Brien S. 2006. Physical fractionation of soil organic matter using sodium hexametaphosphate requires caution. ASA-CSSA-SSSA International Meetings.
- Nadelhoffer K, Emmett B, Gundersen P, Kjonaas O, Koopmans C, Schleppi P, Tietema A, Wright R. 1999. Nitrogen deposition makes a minor contribution to carbon sequestration in temperate forests. *Nature* 398:145–8.
- Norton JM, Firestone MK. 1996. N dynamics in the rhizosphere of *Pinus ponderosa* seedlings. *Soil Biol Biochem* 28:351–62.
- Parton, WJ, Schimel DS, Ojima DS, Cole SV. 1994. A general model for soil organic matter dynamics: sensitivity to litter chemistry, texture and management. In: Quantitative modeling of soil forming processes. Madison (WI): Soil Science Society of America. pp 147–67.
- Pregitzer KS, Zak DR, Burton AJ, Ashby JA, MacDonald NW. 2004. Chronic nitrate additions dramatically increase the export of carbon and nitrogen from northern hardwood ecosystems. *Biogeochemistry* 68:179–97.
- Reich PB, Grigal DF, Aber JD, Gower ST. 1997. Nitrogen mineralization and productivity in 50 hardwood and conifer stands on diverse soils. *Ecology* 78:335–47.
- Six J, Conant RT, Paul EA, Paustian K. 2002. Stabilization mechanisms of soil organic matter: implications for C-saturation of soils. *Plant Soil* 241:155–76.
- Sollins P, Homann P, Caldwell BA. 1996. Stabilization and destabilization of soil organic matter: mechanisms and controls. *Geoderma* 74:65–105.
- Stark JM, Hart SC. 1996. Diffusion technique for preparing salt solutions, Kjeldahl digests, and persulfate digests for nitrogen-15 analysis. *Soil Sci Soc Am J* 60:1846–55.
- Stewart CE, Paustian K, Conant RT, Plante AF, Six J. 2007. Soil carbon saturation: concept, evidence and evaluation. *Biogeochemistry* 86:19–31.
- Vitousek PM, Aber JD, Horwath RW, Likens GE, Matson PA, Schindler DW, Schlesinger WH, Tilman DG. 1997. Human alteration of the global nitrogen cycle: sources and consequences. *Ecol Appl* 7:737–50.
- Zogg GP, Zak DR, Pregitzer KS, Burton AJ. 2000. Microbial immobilization and the retention of anthropogenic nitrate in a northern hardwood forest. *Ecology* 81:1858–66.